ACS APPLIED MATERIALS & INTERFACES

www.acsami.org

Research Article

Color-Changeable Four-Dimensional Printing Enabled with Ultraviolet-Curable and Thermochromic Shape Memory Polymers

Lei Chen, Yiru Zhang, Haitao Ye, Guihui Duan, Huigao Duan, Qi Ge,* and Zhaolong Wang*

Cite This: https://doi.org/10.1021/acsami.1c02656

Read Online

ACCESS | Metrics & More | Article Recommendations | Supporting Information

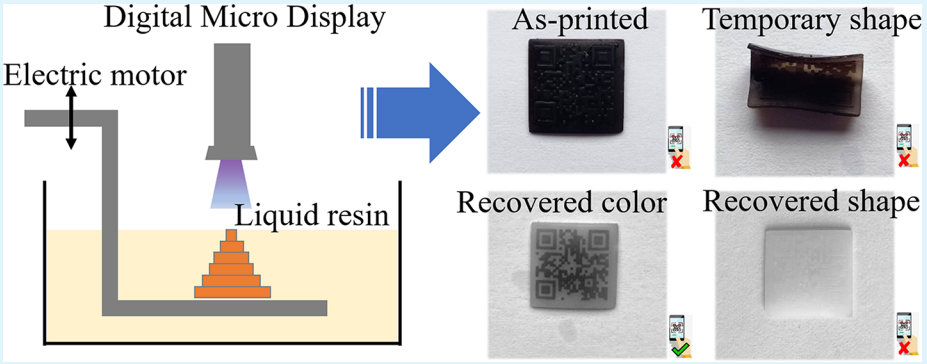

ABSTRACT: Four-dimensional (4D) printing, which enables 3D printed structures to alter shapes over time, is attracting increasing attention because of its exciting potential in various applications. Among all the 4D printing materials, shape memory polymers (SMPs) have a higher stiffness and faster response rate and therefore are considered as one of the most promising 4D printing materials. However, the current studies of SMP-based 4D printing mainly focused on the deformation behavior and structural design of 4D printed structures. An additional function such as color change is desired for 4D printed structure, which would be potentially beneficial to the applications such as anti-counterfeiting, encryption, and bioinspired camouflage. In this paper, we report an ultraviolet (UV)-curable and thermochromic (UVT) SMP system that enables color-changeable 4D printing. The UVT SMP system is acrylate-based, thus highly UV-curable and compatible with PμSL-based high-resolution 3D printing technique. Thermochromism is imparted by adding the thermochromic microcapsules to the UVT SMP system, which allows the printed structures to reversibly change colors upon heating and cooling. To demonstrate its extraordinary thermochromic and mechanical performance, we use UVT SMP to print QR codes and multilevel anti-counterfeiting patterns which can hide the visible information at room temperature and visualize the information by encrypting, decrypting, and encrypting again steps with the shape−color recovery process. The development of UVT SMP will significantly advance current applications of SMP-based 4D printing, especially for anti-counterfeiting and safe data recording.

KEYWORDS: *ultraviolet-curable thermochromic (UVT) SMP, 4D printing, QR code, multilevel anti-counterfeiting, shape memory polymer*

1. INTRODUCTION

Three-dimensional (3D) printing, also known as additive manufacturing, is attracting increasing attention as it allows creation of 3D geometries with precisely prescribed microfeatures to realize new functionalities or improved performance.[1−3] 3D printing technology has been applied to various fields such as drug delivery,[4] electrochemistry,[5] structural mechanics,[6] optical lens,[7,8] biomedical engineering,[9−12] soft robots,[13−17] and so on.[2,18] Digital light processing (DLP)-based 3D printing is considered as a high throughput additive manufacturing technique that employs localized photopolymerization to convert liquid resin to solid patterns. Such a 3D printing technique is capable of creating a variety of highly complex 3D structures from micro- to mesoscales with microscale architecture and submicrometer precision.[3] The recent advances in DLP-based 3D printing lead to various advanced techniques including continuous liquid interface production (CLIP) for fast-speed 3D printing,[19] high-area rapid printing (HARP) for fast-speed large volume 3D printing, and projection micro-stereolithography (PμSL) for high-resolution multiscale 3D printing.[20−23]

Received: February 8, 2021
Accepted: March 26, 2021

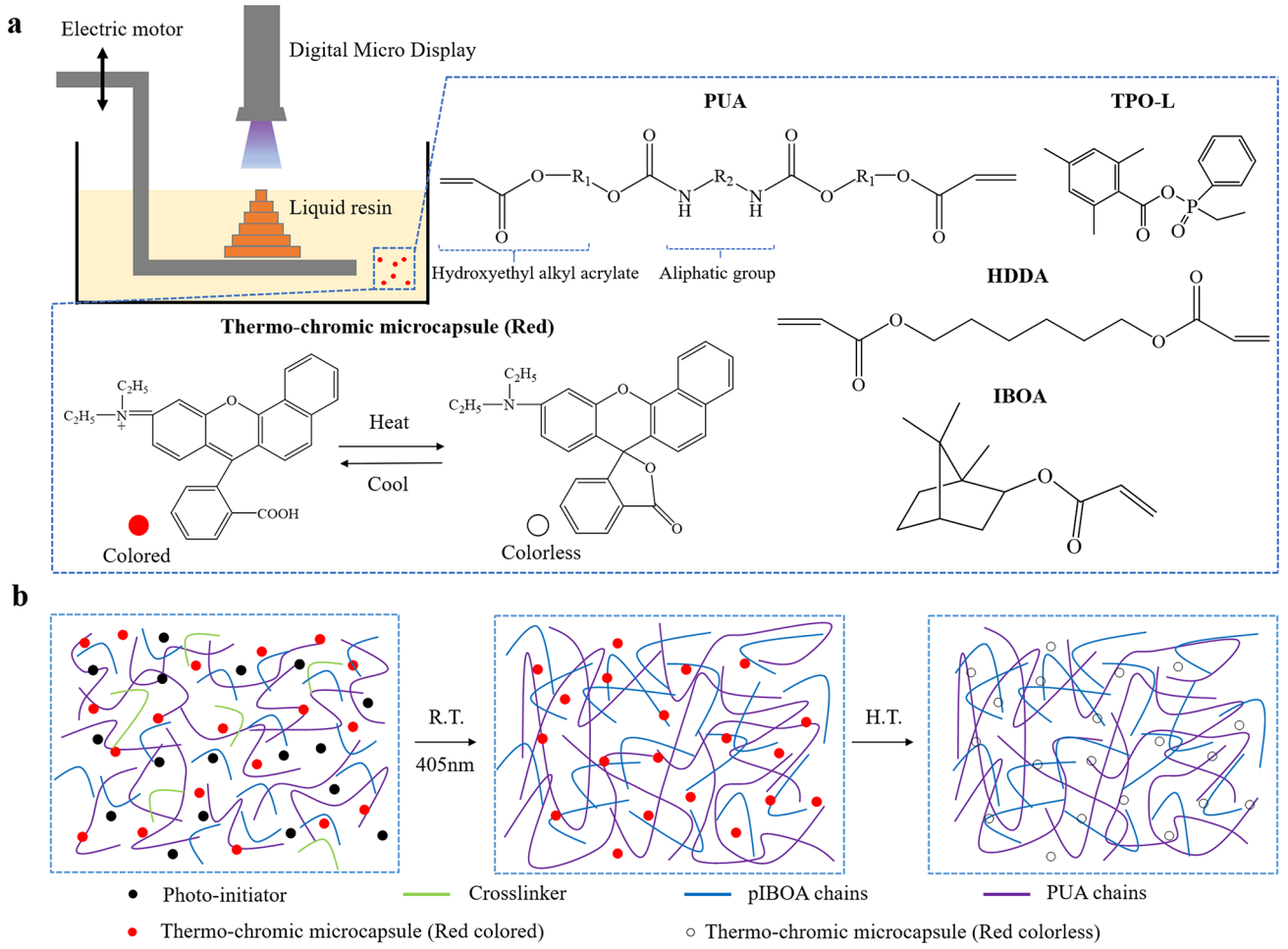

Figure 1. Schematic of the 3D printing technique and the composition of the materials. (a) Schematic diagrams of PμSL 3D printing technique and chemistry of liquid resin in the presence of thermochromic microcapsules (red). (b) Chemical structure evolution of liquid resin during printing process in room temperature and heating after printing.

Along with the rapid advances in 3D printing techniques, researchers are also exploring approaches to generating 3D structures with new functionalities including actuation,[24−27] electric conductivity,[28,29] and biocompatibility.[30,31] Among them, the approach to integrate self-actuating functionality into 3D structures through printing structure with soft active materials such as shape memory polymers (SMP),[32−34] hydrogels,[35−37] and liquid crystal elastomers[38−41] has gained remarkable attention. Such an approach is now well-known as "4D printing", which fabricates 3D structures to change configurations over the fourth dimension "time" in response to environmental stimulus including heat,[33,39] moisture,[36] magnetic field, or electricity.[42] Different from the other two extremely soft SAMs (modulus of hydrogels: ∼1 to 100 kPa;[36,43] modulus of LCEs: ∼100 kPa to ∼MPa[38−41]), SMPs are capable of switching material modulus from a few MPa to a few GPa within 1 min[15] and compatible with various 3D printing technologies. To date, SMP-based 4D printing has been widely applied to numerous areas such as smart device,[32] origami,[24,33] tissue engineering,[44] metamaterial,[45,46] biomedicine,[47−49] and others.[50]

However, those previous 4D printing studies mainly focused on the deformation behavior and structural design of 4D printed structures, which limit the full potential applications of 4D printing. Researchers have developed several additional functions such as color change to broaden the application of SMP-based 4D printing, which exhibit a good effect on color response.[51] However, complicated preparation process and low-resolution fabrication still limit the full potential application of SMPs. Thus, the development of a new kind of functional SMP is desired for 4D printed structures, which would be potentially beneficial to the applications such as anti-counterfeiting, encryption, and bioinspired camouflage.

Herein, we report an ultraviolet (UV)-curable and thermochromic (UVT) SMP system that enables color-changeable 4D printing. The UVT SMP system consists of acrylate-based monomers and cross-linker which make it highly UV-curable, thus compatible with PμSL-based high-resolution multiscale 3D printing. We impart the thermochromism to the SMP system by adding the thermochromic microcapsules which allow the printed structures to reversibly change colors from white to black, red, blue, or yellow upon heating and cooling. The high compatibility of the UVT SMP with PμSL-based 3D printing enables the fabrication of various highly complex 3D structures with high resolution up to 20 μm. More importantly, the structures printed with UVT SMP exhibit outstanding thermochromic ability and shape memory behavior which are highly repeatable. To demonstrate the extraordinary thermochromic and mechanical performance, we use UVT SMP to print QR codes which can hide the visible information at room temperature and visualize the information by encrypting, decrypting, and encrypting again steps with the

https://doi.org/10.1021/acsami.1c02656
ACS Appl. Mater. Interfaces XXXX, XXX, XXX−XXX

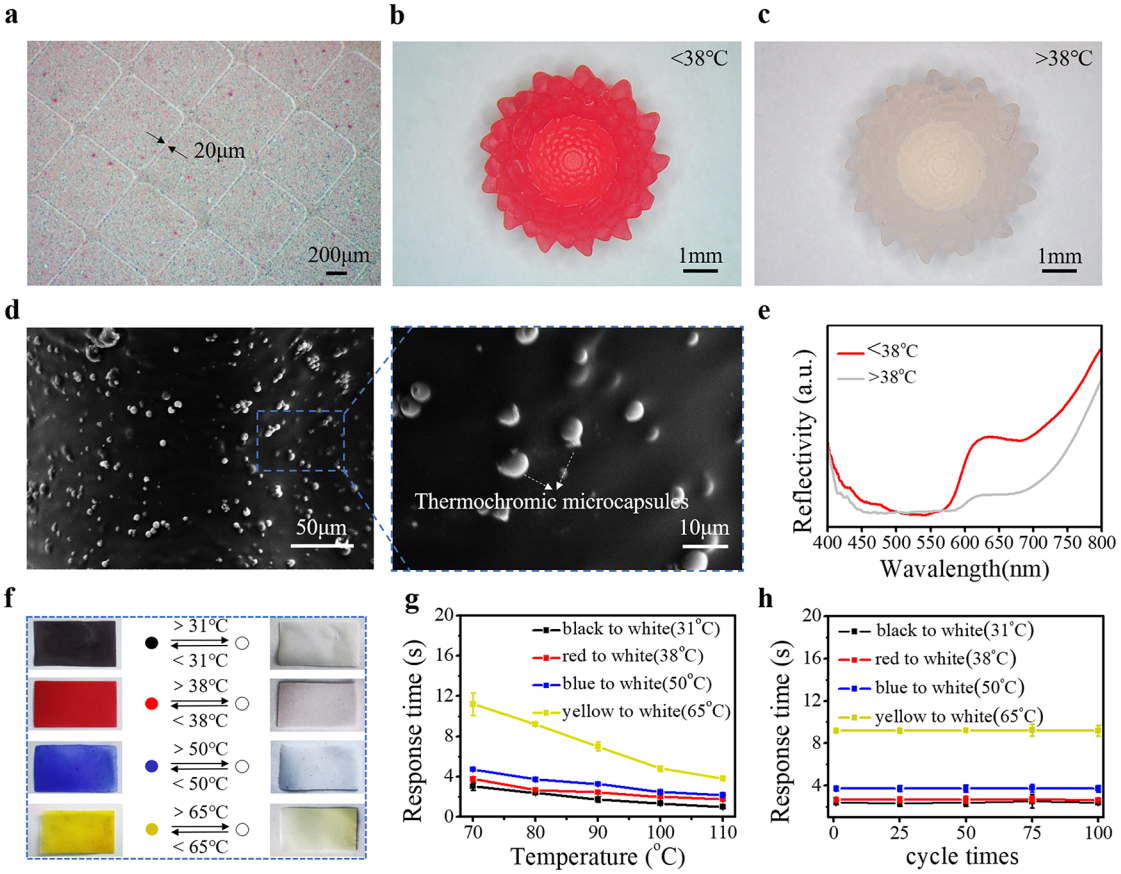

Figure 2. Characteristics of the resin. (a) 3D-printed high-resolution structure using the photocurable liquid resin. (b) Printed sunflower and characteristics of its details with red color at 25 °C. (c) Printed sunflower with white color at 40 °C. (d) SEM images of UVT SMP. (e) Visible spectra of UVT SMP before and after color change. (f) UVT SMPs with different responsive colors and temperatures. (g) Effect of temperature on the color response speed of UVT SMP. (h) Color response speed of UVT SMPs with cycle tests.

shape−color recovery process. Such a triple-deep encryption QR code enabled by reversible complex 3D structure and thermochromics further ensures the security of the information in reality. In addition, the printed high-resolution multilevel anti-counterfeiting patterns using UVT SMP could switch between visible and invisible state in response to stimuli of different temperature, which will significantly advance current applications of SMP-based 4D printing, especially for anti-counterfeiting and safe data recording.

2. RESULTS AND DISCUSSION

2.1. 3D Printing Process and Features. As shown schematically in Figure 1a, we fabricated the high-resolution and highly complex 3D structures and devices with UVT SMP by a commercial PμSL-based 3D printer (BMF, S140, China). A computer-aided design (CAD) 3D model was firstly sliced into a series of closed spaced two-dimensional (2D) digital images. Then, these 2D images were transmitted to a digital micromirror device (DMD) to modulate ultraviolet (UV) light generated from a light-emitting diode (LED) array. The patterned UV light then illuminated onto the surface of a UV-curable liquid resin to trigger the localized photopolymerization. Once the exposed resin was solidified to a layer of the corresponding pattern, the substrate on which the fabricated structure rested was lowered by the electric motor. This process proceeded iteratively until the entire structure was fabricated (Figure S1, Supporting Information). The 3D printed structure was sonicated with ethanol to remove uncured oligomer and monomer followed by a second stage cure in a UV oven after the printing process.

As illustrated in Figure 1b, we prepared the UVT SMP liquid resin by mixing aliphatic polyurethane acrylate (PUA, as oligomer), isobornyl acrylate (IBOA, as monomer), and 1, 6-hexanediol diacrylate (HDDA, as cross-linker). Ethyl(2,4,6-trimethylbenzoyl) phenylphosphinate (TPO-L) was added into the liquid resin and works as free radical photoinitiator to initiate the copolymerization of PUA oligomer, IBOA monomer, and HDDA cross-linker to obtain shape memory structures. The solidified polymers with different weight contents of PUA and IBOA after polymerization were verified by the Fourier transform infrared (FTIR) spectrum shown in Figure S2. In addition, thermochromic microcapsules were added into the UV-curable liquid resin to endow the solidified polymer with superior thermochromic properties (Figure 1b). The molecular structures of thermochromic microcapsule (red TF-R1) and thermochromic mechanism are described in Figure 1a and Figure S3. Details about the liquid resin preparation are provided in the Experimental Section.

2.2. Thermochromic Performance. The liquid resin has a good compatibility with the PμSL-based high-resolution 3D printing technique. By use of the present liquid resin, a high-resolution structure was firstly fabricated (Figure 2a). We can achieve a high printing resolution up to 20 μm. As depicted in Figure 2b and Figure S4, the printed sunflower and flower petals also showed excellent printing resolution and smooth surface, indicating the ability of the resin to fabricate complex

https://doi.org/10.1021/acsami.1c02656
ACS Appl. Mater. Interfaces XXXX, XXX, XXX−XXX

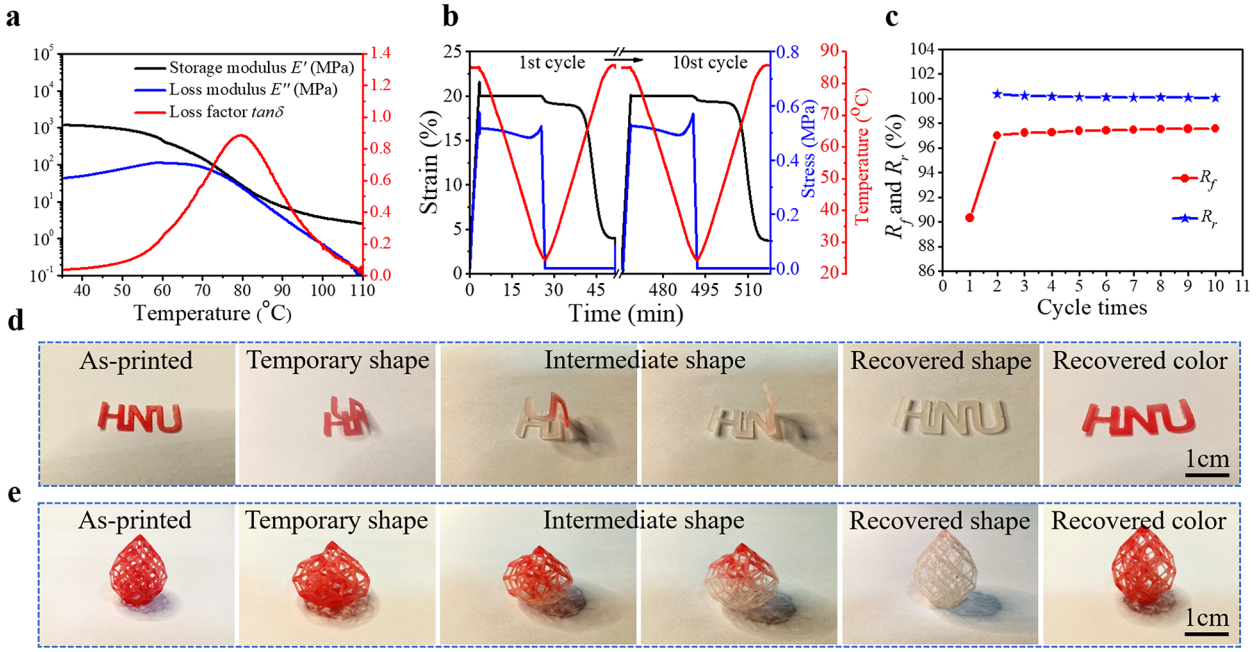

Figure 3. Shape recovery properties of the UVT SMP. (a) DMA curves of UVT SMP. (b) Shape memory cycle test. (c) Shape fixity (R_f) and shape recovery (R_r) during ten cycles. (d) 3D printed "HNU" letters. (e) 3D printed hollow structure with good recovery performance.

structures. In addition, the original color of printed sunflower and flower petals was red at room temperature, while the UVT SMP exhibited discoloration from red to white (Figure 2c and Figure S4) with the temperature increasing to a threshold temperature of 38 °C. The thermochromic property of the polymer could be ascribed to the distribution of thermochromic microcapsules (red to white with a threshold temperature of 38 °C) in it. Scanning electron microscopy (SEM) images demonstrated the distribution of microcapsules (Figure 2d), and the polymer without microcapsules was used for comparison (Figure S5). It was worth noted that microcapsules with a diameter of 3−5 μm distributed well in polymer without any agglomerate. To further demonstrate the thermochromic performance of UVT SMP, a visible spectrum of polymer with microcapsules on a UV−vis spectrophotometer from 400 nm to 800 nm was obtained. The results showed that wavelengths corresponding to a peak from 635 to 700 nm disappeared gradually with the temperature increasing to its threshold temperature of 38 °C (red to white, Figure 2e).

UVT SMPs with different responsive color and temperature were also demonstrated in Figure 2f. It could be observed that the color change of UVT SMPs includes two processes of fading and coloring with different response temperature. The thermochromic microcapsules changed from a low-temperature stable state to a high-temperature state when heated, resulting in the change of the absorbing light wavelength, which was also the change of its color. After cooling, the color returned to its original state. Figure 2g shows the effect of the temperature on the color response speed. It could be seen that the response time decreased with the increase of the temperature from 70 to 110 °C. Meanwhile, the color response speed of UVT SMPs for at least 100 cycles was almost the same as the original one at 80 °C (Figure 2h and Figure S4), indicating great stability of the color response effect.

2.3. Shape Memory Performance. Differential scanning calorimetry (DSC) tests were firstly applied to study thermal properties of UVT SMP. The results showed that its glass transition temperature (T_g) could be tuned from 74.2 to 81.7 °C with the increase of the weight content of IBOA. Meanwhile, thermal gravimetric (TG) tests demonstrated a high start degrading temperature of UVT SMP, indicating that there was no thermal decomposition during the deformation process around the glass transition in the next shape memory tests (Figure S6).

The mechanical properties of UVT SMP were also evaluated by uniaxial tensile tests. Figure S7 shows the strain−stress curves of UVT SMP modified with different weight contents of PUA and IBOA. The results indicated that UVT SMP modified with a higher weight content of IBOA showed a significant increase in stress related to increasing toughness. In addition, tensile tests of UVT SMP with a 60% weight fraction of IBOA at different temperatures were carried out, and the results showed that the UVT SMP had a higher break elongation with a higher temperature (Figure S7).

To gain further insights into shape memory properties of UVT SMP, we used the printed sample with 60% weight fraction of IBOA to demonstrate the shape memory effect. Dynamic thermomechanical analysis (DMA) measurement was applied to determine the storage modulus (E'), loss modulus (E''), and loss factor (tan δ). As shown in Figure 3a, the storage modulus of UVT SMP decreased with the increase of the temperature, and the glass transition temperature (T_g) of UVT SMP determined from the peak of tan δ curve was 80 °C, which was consistent with the result in DSC test. The shape memory performance of UVT SMP was investigated by shape memory cycles test to quantitatively evaluate the value of shape fixity (R_f) and shape recovery (R_r) ratios. As shown in Figure 3b, the shape memory cycle test involved the following steps. First, a printed sample was stretched with external force at a deformation temperature (85 °C) until the stress reached 0.5 MPa, and the strain was recorded as ε_m at the end of this step. Second, the printed sample was cooled to 25 °C with the external force. Then, the external force was removed at 25 °C, and the strain was recorded as ε_u at the end of this step.

https://doi.org/10.1021/acsami.1c02656
ACS Appl. Mater. Interfaces XXXX, XXX, XXX−XXX

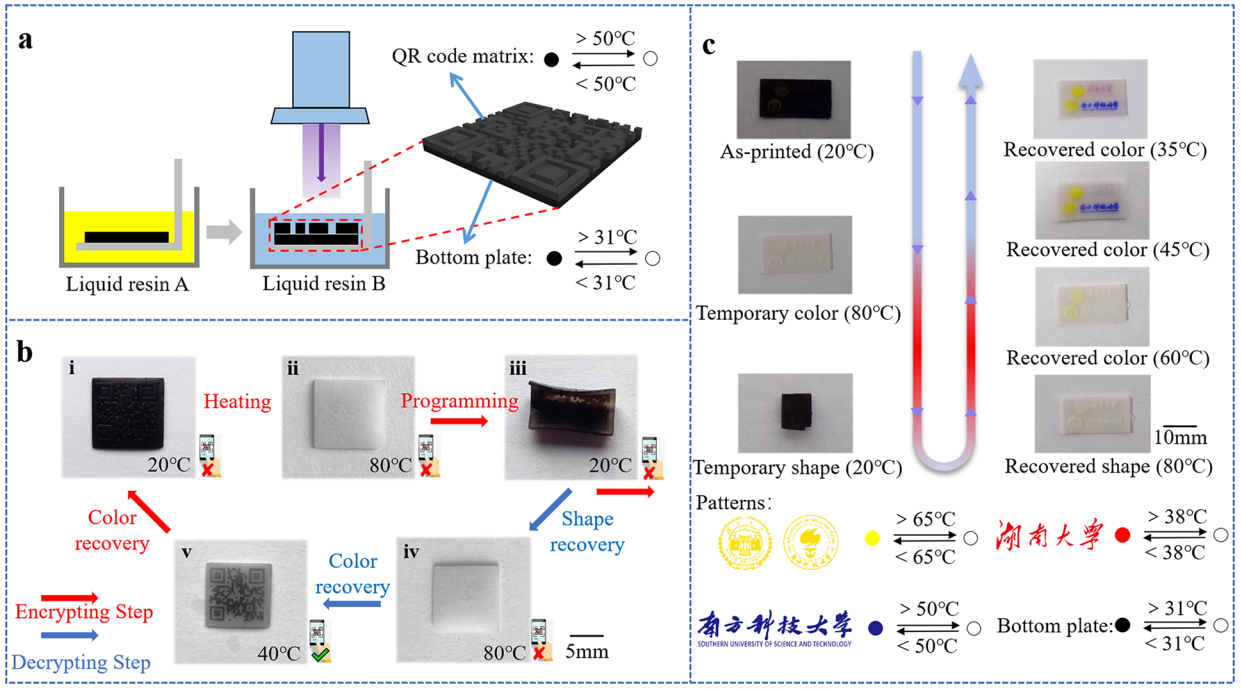

Figure 4. Triple-deep encryption enabled by reversible complex 3D structure made of the present resin. (a) Schematic of the 3D printed QR code by liquid resin. (b) Encrypting, decrypting, and encrypting again steps of the QR code structure by shape−color recovery. (c) Printed high-resolution anti-counterfeiting patterns with multilevel anti-counterfeit protection.

Finally, the printed sample was heated to 85 °C again to recover its original shape, and the strain of the printed sample was recorded as ε_r. The change of strain is the same in each cycle during the shape memory cycles test, except for a small residue strain of about 3.98% can be seen after the first cycle (Figure S8). Such irreversible deformation may be attributed to directional rearrangement of polymer chains upon the external force.[52,53] The shape fixity (R_f) and shape recovery (R_r) were determined by:[53,54]

$$R_f(N) = \frac{\varepsilon_u(N)}{\varepsilon_m(N)} \times 100\% \quad (1)$$

$$R_r(N) = \frac{\varepsilon_m(N) - \varepsilon_r(N)}{\varepsilon_m(N) - \varepsilon_r(N-1)} \times 100\% \quad (2)$$

The shape memory cycle test was repeated 10 times, and the values of shape fixity (R_f) and shape recovery (R_r) are shown in Figure 3c. The average shape fixity (R_f) and shape recovery (R_r) were 96.7% and 100%, respectively, indicating excellent repeated shape memory properties of UVT SMP. We further fabricated a structure of the letters "HNU" as well as a hollow structure containing microcapsules (red to white with a threshold temperature of 38 °C), and the shape memory and thermochromic process of 3D-printed samples were shown in Figures 3d and 3e, respectively. Meanwhile, a series of complex structures were printed to demonstrate the shape−color memory behavior of UVT SMP, and the thermochromic ability and outstanding shape memory behavior enabled great application as a gripper which was used to grab or release objects (Figures S8 and S9, Video S1, and Video S2).

2.4. 3D Multilevel Anti-counterfeiting. Such a marvelous shape memory behavior, good thermochromic properties, and superhigh-resolution features of the UVT SMP imply great potential for practical applications in anti-counterfeiting protection and security information recording. The QR code could be coded by the difference and arrangement of colors in both of the horizontal and vertical directions. We firstly printed a high-resolution QR code structure by automating the present liquid resin exchange during the printing process (Figure 4a). The printed QR code structure was combined with a cubic bottom plate containing microcapsules (black to white at a threshold temperature of 31 °C, printed by liquid resin A) and QR code-shape matrix containing microcapsules (black to white at a threshold temperature of 50 °C, printed by liquid resin B). As shown in Figure 4b(i), the QR code was black, which could be used to hide the information at room temperature. Then, the printed QR code was heated to 80 °C and cooled to 20 °C afterward to further program its complex shape under external force as double encryption (Figure 4b(ii,iii)). For the purpose of decrypting the QR code, the QR code was heated to 80 °C to recover to its original shape and complete the discoloration of the whole structure. Then, it was cooled down to 40 °C to recover the original color of the QR code-shape matrix as decryption (Figure 4b(iv,v) and Video S3). The printed QR code was visible, which could be scanned to browse the official web site of Hunan University (Video S4). Furthermore, the QR code was cooled to 20 °C to recover the original color of the cube-shaped bottom plate as encryption again, which could hide the visible information again and improve the security of anti-counterfeit labels (Figure 4b(vi) and Figure S10). For the high-resolution 3D structures which can be folded, the visibility of the information within a certain temperature range (20−40 °C in this study) promises the 3D printed QR code great potential in the field of deep anti-counterfeiting.

In addition, we printed high-resolution anti-counterfeiting patterns on the bottom plate with different thermoresponsive liquid resins. As shown in Figure 4c, the patterns were not readable at either 20 or 80 °C. However, when the printed

https://doi.org/10.1021/acsami.1c02656
ACS Appl. Mater. Interfaces XXXX, XXX, XXX−XXX

structure completed a shape memory process, the high-quality patterns became visible and diverse in the temperature range 31−65 °C. Specifically, at 60 °C, only the yellow pattern was visible because the temperature exceeded the threshold temperature of 31 °C (black to white), 38 °C (red to white), and 50 °C (blue to white) but was below the threshold temperature of 65 °C (yellow to white). Similarly, the yellow and blue patterns were visible while the red pattern was invisible at 38 °C, and both the yellow blue and red patterns were visible at 35 °C. All the patterns disappeared again after the temperature was cooled down to 20 °C (Video S5). Thus, the outstanding performance of UVT SMP based on 3D printing developed in this work demonstrated great potential for practical applications related to anti-counterfeiting and safe data recording.

3. CONCLUSION

We developed a new reversible ultraviolet (UV)-curable and thermochromic (UVT) SMP based on a PμSL 3D printing technique. The photocurable resin and thermochromic microcapsule composites for 3D printing exhibited high resolution (up to 20 μm) and marvelous ability to fabricate complex structures, and thermochromic microcapsules distributed well in polymer without any agglomeration. The present polymer also exhibited thermochromic ability, outstanding shape memory behavior, and repeated response performance (96.7% of shape fixity (R_f) and 100% of shape recovery (R_r) during 10 cycles). The printed bionic gripper made of the present resin could grab and release an object with shape−color change, which can be used to prejudge the deformation of polymer. Most importantly, the printed high-resolution QR code could hide the visible information at room temperature and visualize information by encrypting, decrypting, and encrypting again steps with the shape−color recovery process. The printed high-resolution multilevel anti-counterfeiting patterns using the thermochromic shape memory polymer could switch between the visible and invisible states in a temperature range. We believe that this thermochromic shape memory polymer based on 3D printing paves a new way to a wide variety of practical applications such as high-precision devices, soft robots, bionic devices, intelligent anti-counterfeiting, and safe data recording, especially for the triple-deep encryption and multilevel security protection enabled by coexistence of marvelous shape memory and thermochromics of the proposed polymer.

■ ASSOCIATED CONTENT

Supporting Information

The Supporting Information is available free of charge at https://pubs.acs.org/doi/10.1021/acsami.1c02656.

Experimental section; material used in liquid resin; PμSL printing parameters; 3D printing process; FTIR spectrum; molecular structures and thermochromic mechanisms; thermochromic ability; SEM images; TG-DSC tests; uniaxial tensile tests; shape−color memory process; 3D printed bionic gripper; schematic diagram of encrypting, decrypting, and encrypting again steps of a 3D printed QR code structure (PDF)

Video S1: shape−color memory process of 3D printed "HNU" letters (MP4)

Video S2: shape−color memory process of 3D printed hollow structure (MP4)

Video S3: decrypting and encrypting again steps of 3D printed QR code structure with shape−color recovery process (MP4)

Video S4: scanning the QR code to browse official web site of Hunan University (MP4)

Video S5: printed high-resolution anti-counterfeiting patterns from 80 to 20 °C (MP4)

■ AUTHOR INFORMATION

Corresponding Authors

Zhaolong Wang − *National Research Center for High-Efficiency Grinding, College of Mechanical and Vehicle Engineering, Hunan University, Changsha 410082, P. R. China;* orcid.org/0000-0003-2967-4546; Email: zhaolongwang@hnu.edu.cn

Qi Ge − *Department of Mechanical and Energy Engineering, Southern University of Science and Technology, Shenzhen 518055, P. R. China;* orcid.org/0000-0002-8666-8532; Email: geq@sustech.edu.cn

Authors

Lei Chen − *National Research Center for High-Efficiency Grinding, College of Mechanical and Vehicle Engineering, Hunan University, Changsha 410082, P. R. China*

Yiru Zhang − *National Research Center for High-Efficiency Grinding, College of Mechanical and Vehicle Engineering, Hunan University, Changsha 410082, P. R. China*

Haitao Ye − *Department of Mechanical and Energy Engineering, Southern University of Science and Technology, Shenzhen 518055, P. R. China*

Guihui Duan − *National Research Center for High-Efficiency Grinding, College of Mechanical and Vehicle Engineering, Hunan University, Changsha 410082, P. R. China*

Huigao Duan − *National Research Center for High-Efficiency Grinding, College of Mechanical and Vehicle Engineering, Hunan University, Changsha 410082, P. R. China;* orcid.org/0000-0002-7016-6343

Complete contact information is available at: https://pubs.acs.org/10.1021/acsami.1c02656

Author Contributions

L.C., Y.Z., and H.Y. contributed equally to this work. Z.W, L.C. and Y.Z. conceived the project, designed the experiments, and carried out the experimental work. H.Y. measured the shape recovery properties of the polymer. G.D. helped design the project. L.C., Y.Z., Z.W., H.D. and Q.G. analyzed the data and wrote the manuscript. Z.W., H.D. and Q.G. supervised the whole project. All the authors discussed the results and commented on the manuscript.

Notes

The authors declare no competing financial interest.

■ ACKNOWLEDGMENTS

This work was supported by the Key-Area Research and Development Program of Guangdong Province (2020B090923003) and the National Natural Science Foundation of China (52006056, 51722503, and 51621004). The project was also supported in part by Science and Technology Bureau Foundation of Changsha City (kh1904005) and the Natural Science Foundation of Hunan through Grant 2020JJ3012.

REFERENCES

(1) Walker, D. A.; Hedrick, J. L.; Mirkin, C. A. Rapid, large-volume, thermally controlled 3D printing using a mobile liquid interface. *Science* **2019**, *366*, 360−364.

(2) Ligon, S. C.; Liska, R.; Stampfl, J.; Gurr, M.; Mülhaupt, R. Polymers for 3D printing and customized additive manufacturing. *Chem. Rev.* **2017**, *117*, 10212−10290.

(3) Ge, Q.; Li, Z.; Wang, Z.; Kowsari, K.; Zhang, W.; He, X.; Zhou, J.; Fang, N. X. Projection micro stereolithography based 3D printing and its applications. *Int. J. Extrem. Manuf.* **2020**, *2*, 022004.

(4) Xing, J.-F.; Zheng, M.-L.; Duan, X.-M. Two-photon polymerization microfabrication of hydrogels: an advanced 3D printing technology for tissue engineering and drug delivery. *Chem. Soc. Rev.* **2015**, *44*, 5031−5039.

(5) Ambrosi, A.; Pumera, M. 3D-printing technologies for electrochemical applications. *Chem. Soc. Rev.* **2016**, *45*, 2740−2755.

(6) Kang, J.; Shangguan, H.; Deng, C.; Hu, Y.; Yi, J.; Wang, X.; Zhang, X.; Huang, T. Additive manufacturing-driven mold design for castings. *Addit. Manuf.* **2018**, *22*, 472−478.

(7) Gissibl, T.; Thiele, S.; Herkommer, A.; Giessen, H. Sub-micrometre accurate free-form optics by three-dimensional printing on single-mode fibres. *Nat. Commun.* **2016**, *7*, 1−9.

(8) Yuan, C.; Kowsari, K.; Panjwani, S.; Chen, Z.; Wang, D.; Zhang, B.; Ng, C. J.; Alvarado, P. V. y; Ge, Q. Ultrafast Three-Dimensional Printing of Optically Smooth Microlens Arrays by Oscillation-Assisted Digital Light Processing. *ACS Appl. Mater. Interfaces* **2019**, *11*, 40662−40668.

(9) Noor, N.; Shapira, A.; Edri, R.; Gal, I.; Wertheim, L.; Dvir, T. 3D printing of personalized thick and perfusable cardiac patches and hearts. *Adv. Sci.* **2019**, *6*, 1900344.

(10) Kang, H.-W.; Lee, S. J.; Ko, I. K.; Kengla, C.; Yoo, J. J.; Atala, A. A 3D bioprinting system to produce human-scale tissue constructs with structural integrity. *Nat. Biotechnol.* **2016**, *34*, 312.

(11) Kim, S. H.; Yeon, Y. K.; Lee, J. M.; Chao, J. R.; Lee, Y. J.; Seo, Y. B.; Sultan, M. T.; Lee, O. J.; Lee, J. S.; Yoo, J. J.; Park, C. C.; et al. Precisely printable and biocompatible silk fibroin bioink for digital light processing 3D printing. *Nat. Commun.* **2018**, *9*, 1−14.

(12) Lee, A.; Hudson, A.; Shiwarski, D.; Tashman, J.; Hinton, T.; Yerneni, S.; Bliley, J.; Campbell, P.; Feinberg, A. W. 3D bioprinting of collagen to rebuild components of the human heart. *Science* **2019**, *365*, 482−487.

(13) Kim, Y.; Yuk, H.; Zhao, R.; Chester, S. A.; Zhao, X. Printing ferromagnetic domains for untethered fast-transforming soft materials. *Nature* **2018**, *558*, 274−279.

(14) Wehner, M.; Truby, R. L.; Fitzgerald, D. J.; Mosadegh, B.; Whitesides, G. M.; Lewis, J. A.; Wood, R. J. An integrated design and fabrication strategy for entirely soft, autonomous robots. *Nature* **2016**, *536*, 451−455.

(15) Zhang, Y. F.; Zhang, N.; Hingorani, H.; Ding, N.; Wang, D.; Yuan, C.; Zhang, B.; Gu, G.; Ge, Q. Fast-Response, Stiffness-Tunable Soft Actuator by Hybrid Multimaterial 3D Printing. *Adv. Funct. Mater.* **2019**, *29*, 1806698.

(16) Zhang, Y. F.; Ng, C. J. X.; Chen, Z.; Zhang, W.; Panjwani, S.; Kowsari, K.; Yang, H. Y.; Ge, Q. Miniature Pneumatic Actuators for Soft Robots by High-Resolution Multimaterial 3D Printing. *Adv. Mater. Technol.* **2019**, *4*, 1900427.

(17) Patel, D. K.; Sakhaei, A. H.; Layani, M.; Zhang, B.; Ge, Q.; Magdassi, S. Highly stretchable and UV curable elastomers for digital light processing based 3D printing. *Adv. Mater.* **2017**, *29*, 1606000.

(18) Layani, M.; Wang, X.; Magdassi, S. Novel materials for 3D printing by photopolymerization. *Adv. Mater.* **2018**, *30*, 1706344.

(19) Tumbleston, J. R.; Shirvanyants, D.; Ermoshkin, N.; Janusziewicz, R.; Johnson, A. R.; Kelly, D.; Chen, K.; Pinschmidt, R.; Rolland, J. P.; Ermoshkin, A.; Samulski, E. T.; DeSimone, J. M. Continuous liquid interface production of 3D objects. *Science* **2015**, *347*, 1349−1352.

(20) Zheng, X.; Lee, H.; Weisgraber, T. H.; Shusteff, M.; DeOtte, J.; Duoss, E. B.; Kuntz, J. D.; Biener, M. M.; Ge, Q.; Jackson, J. A.; Kucheyev, S. O.; Fang, N. X.; Spadaccini, C. M. Ultralight, ultrastiff mechanical metamaterials. *Science* **2014**, *344*, 1373−1377.

(21) Zheng, X.; Smith, W.; Jackson, J.; Moran, B.; Cui, H.; Chen, D.; Ye, J.; Fang, N.; Rodriguez, N.; Weisgraber, T.; Spadaccini, C. M. Multiscale metallic metamaterials. *Nat. Mater.* **2016**, *15*, 1100−1106.

(22) Sun, C.; Fang, N.; Wu, D. M.; Zhang, X. Projection micro-stereolithography using digital micro-mirror dynamic mask. *Sens. Actuators, A* **2005**, *121*, 113−120.

(23) Zheng, X. Y.; Deotte, J.; Alonso, M. P.; Farquar, G. R.; Weisgraber, T. H.; Gemberling, S.; Lee, H.; Fang, N.; Spadaccini, C. M. Design and optimization of a light-emitting diode projection micro-stereolithography three-dimensional manufacturing system. *Rev. Sci. Instrum.* **2012**, *83*, 125001.

(24) Ge, Q.; Dunn, C. K.; Qi, H. J.; Dunn, M. L. Active origami by 4D printing. *Smart Mater. Struct.* **2014**, *23*, 094007.

(25) Ge, Q.; Qi, H. J.; Dunn, M. L. Active materials by four-dimension printing. *Appl. Phys. Lett.* **2013**, *103*, 131901.

(26) Ge, Q.; Sakhaei, A. H.; Lee, H.; Dunn, C. K.; Fang, N. X.; Dunn, M. L. Multimaterial 4D Printing with Tailorable Shape Memory Polymers. *Sci. Rep.* **2016**, *6*, 31110.

(27) Raviv, D.; Zhao, W.; McKnelly, C.; Papadopoulou, A.; Kadambi, A.; Shi, B.; Hirsch, S.; Dikovsky, D.; Zyracki, M.; Olguin, C.; Raskar, R.; Tibbits, S. Active Printed Materials for Complex Self-Evolving Deformations. *Sci. Rep.* **2014**, *4*, 7422.

(28) Zhang, B.; Li, S. Y.; Hingorani, H.; Serjouei, A.; Larush, L.; Pawar, A. A.; Goh, W. H.; Sakhaei, A. H.; Hashimoto, M.; Kowsari, K.; Magdassi, S.; Ge, Q. Highly stretchable hydrogels for UV curing based high-resolution multimaterial 3D printing. *J. Mater. Chem. B* **2018**, *6*, 3246−3253.

(29) Muth, J. T.; Vogt, D. M.; Truby, R. L.; Menguc, Y.; Kolesky, D. B.; Wood, R. J.; Lewis, J. A. Embedded 3D Printing of Strain Sensors within Highly Stretchable Elastomers. *Adv. Mater.* **2014**, *26*, 6307−6312.

(30) Grigoryan, B.; Paulsen, S. J.; Corbett, D. C.; Sazer, D. W.; Fortin, C. L.; Zaita, A. J.; Greenfield, P. T.; Calafat, N. J.; Gounley, J. P.; Ta, A. H.; Johansson, F.; Randles, A.; Rosenkrantz, J. E.; Louis-Rosenberg, J. D.; Galie, P. A.; Stevens, K. R.; Miller, J. S. Multivascular networks and functional intravascular topologies within biocompatible hydrogels. *Science* **2019**, *364*, 458−464.

(31) Koffler, J.; Zhu, W.; Qu, X.; Platoshyn, O.; Dulin, J. N.; Brock, J.; Graham, L.; Lu, P.; Sakamoto, J.; Marsala, M.; Chen, S.; Tuszynski, M. H. Biomimetic 3D-printed scaffolds for spinal cord injury repair. *Nat. Med.* **2019**, *25*, 263−269.

(32) Zarek, M.; Layani, M.; Cooperstein, I.; Sachyani, E.; Cohn, D.; Magdassi, S. 3D Printing of Shape Memory Polymers for Flexible Electronic Devices. *Adv. Mater.* **2016**, *28*, 4449−4454.

(33) Ding, Z.; Yuan, C.; Peng, X.; Wang, T.; Qi, H. J.; Dunn, M. L. Direct 4D printing via active composite materials. *Sci. Adv.* **2017**, *3*, e1602890.

(34) Yang, H.; Leow, W. R.; Wang, T.; Wang, J.; Yu, J.; He, K.; Qi, D.; Wan, C.; Chen, X. 3D Printed Photoresponsive Devices Based on Shape Memory Composites. *Adv. Mater.* **2017**, *29*, 1701627.

(35) Mao, Y.; Ding, Z.; Yuan, C.; Ai, S.; Isakov, M.; Wu, J.; Wang, T.; Dunn, M. L.; Qi, H. J. 3D Printed Reversible Shape Changing Components with Stimuli Responsive Materials. *Sci. Rep.* **2016**, *6* (1), 24761.

(36) Gladman, A. S.; Matsumoto, E. A.; Nuzzo, R. G.; Mahadevan, L.; Lewis, J. A. Biomimetic 4D printing. *Nat. Mater.* **2016**, *15*, 413−418.

(37) Zhao, Z.; Kuang, X.; Yuan, C.; Qi, H. J.; Fang, D. Hydrophilic/Hydrophobic Composite Shape-Shifting Structures. *ACS Appl. Mater. Interfaces* **2018**, *10*, 19932−19939.

(38) Ambulo, C. P.; Burroughs, J. J.; Boothby, J. M.; Kim, H.; Shankar, M. R.; Ware, T. H. Four-dimensional Printing of Liquid Crystal Elastomers. *ACS Appl. Mater. Interfaces* **2017**, *9*, 37332−37339.

(39) Kotikian, A.; Truby, R. L.; Boley, J. W.; White, T. J.; Lewis, J. A. 3D Printing of Liquid Crystal Elastomeric Actuators with Spatially Programed Nematic Order. *Adv. Mater.* **2018**, *30*, 1706164.

https://doi.org/10.1021/acsami.1c02656
ACS Appl. Mater. Interfaces XXXX, XXX, XXX−XXX

(40) Davidson, E. C.; Kotikian, A.; Li, S.; Aizenberg, J.; Lewis, J. A. 3D Printable and Reconfigurable Liquid Crystal Elastomers with Light-Induced Shape Memory via Dynamic Bond Exchange. *Adv. Mater.* **2020**, *32*, 1905682.
(41) Saed, M. O.; Ambulo, C. P.; Kim, H.; De, R.; Raval, V.; Searles, K.; Siddiqui, D. A.; Cue, J. M. O.; Stefan, M. C.; Shankar, M. R.; Ware, T. H. Molecularly-Engineered, 4D-Printed Liquid Crystal Elastomer Actuators. *Adv. Funct. Mater.* **2019**, *29*, 1806412.
(42) Rodriguez, J. N.; Zhu, C.; Duoss, E. B.; Wilson, T. S.; Spadaccini, C. M.; Lewicki, J. P. Shape-morphing composites with designed micro-architectures. *Sci. Rep.* **2016**, *6*, 27933.
(43) Bakarich, S. E.; Gorkin, R., III; in het Panhuis, M.; Spinks, G. M. 4D Printing with Mechanically Robust, Thermally Actuating Hydrogels. *Macromol. Rapid Commun.* **2015**, *36*, 1211−1217.
(44) Villar, G.; Graham, A. D.; Bayley, H. A tissue-like printed material. *Science* **2013**, *340*, 48−52.
(45) Tao, R.; Xi, L.; Wu, W.; Li, Y.; Liao, B.; Liu, L.; Leng, J.; Fang, D. 4D printed multi-stable metamaterials with mechanically tunable performance. *Compos. Struct.* **2020**, *252*, 112663.
(46) Yang, C.; Boorugu, M.; Dopp, A.; Ren, J.; Martin, R.; Han, D.; Choi, W.; Lee, H. 4D printing reconfigurable, deployable and mechanically tunable metamaterials. *Mater. Horiz.* **2019**, *6*, 1244−1250.
(47) Wei, H.; Zhang, Q.; Yao, Y.; Liu, L.; Liu, Y.; Leng, J. Direct-Write Fabrication of 4D Active Shape-Changing Structures Based on a Shape Memory Polymer and Its Nanocomposite. *ACS Appl. Mater. Interfaces* **2017**, *9*, 876−883.
(48) Lin, C.; Lv, J.; Li, Y.; Zhang, F.; Li, J.; Liu, Y.; Liu, L.; Leng, J. 4D-Printed Biodegradable and Remotely Controllable Shape Memory Occlusion Devices. *Adv. Funct. Mater.* **2019**, *29*, 1906569.
(49) Zhang, B.; Zhang, W.; Zhang, Z.; Zhang, Y. F.; Hingorani, H.; Liu, Z.; Liu, J.; Ge, Q. Self-Healing Four-Dimensional Printing with an Ultraviolet Curable Double-Network Shape Memory Polymer System. *ACS Appl. Mater. Interfaces* **2019**, *11*, 10328−10336.
(50) Kuang, X.; Roach, D. J.; Wu, J.; Hamel, C. M.; Ding, Z.; Wang, T.; Dunn, M. L.; Qi, H. J. Advances in 4D Printing: Materials and Applications. *Adv. Funct. Mater.* **2019**, *29*, 1805290.
(51) Wang, J.; Wang, Z.; Song, Z.; Ren, L.; Liu, Q.; Ren, L. Biomimetic Shape-Color Double-Responsive 4D Printing. *Adv. Mater. Technol.* **2019**, *4*, 1900293.
(52) Yu, R.; Yang, X.; Zhang, Y.; Zhao, X.; Wu, X.; Zhao, T.; Zhao, Y.; Huang, W. Three-dimensional printing of shape memory composites with epoxy-acrylate hybrid photopolymer. *ACS Appl. Mater. Interfaces* **2017**, *9*, 1820−1829.
(53) Zhao, T.; Yu, R.; Li, X.; Cheng, B.; Zhang, Y.; Yang, X.; Zhao, X.; Zhao, Y.; Huang, W. 4D printing of shape memory polyurethane via stereolithography. *Eur. Polym. J.* **2018**, *101*, 120−126.
(54) Chen, K.; Kuang, X.; Li, V.; Kang, G.; Qi, H. J. Fabrication of tough epoxy with shape memory effects by UV-assisted direct-ink write printing. *Soft Matter* **2018**, *14*, 1879−1886.

https://doi.org/10.1021/acsami.1c02656
ACS Appl. Mater. Interfaces XXXX, XXX, XXX−XXX